

# Lambda baryon production in heavy-ion collisions at the NA61/SHINE experiment

---

**Yuliia Balkova<sup>a,\*</sup> for the NA61/SHINE collaboration**

<sup>a</sup>*University of Silesia,*

*12 Bankowa str., 40-007 Katowice, Poland*

*E-mail: [yuliia.balkova@cern.ch](mailto:yuliia.balkova@cern.ch)*

Strangeness production in heavy-ion collisions is a longstanding and actively researched topic, offering crucial insights into the properties of strongly interacting matter. The NA61/SHINE experiment at CERN SPS North Area is one of the leading experiments in this field, focusing on measuring hadron production in a wide range of collision energies and system sizes.

This talk emphasizes the significance of measuring strangeness production with respect to the onset of deconfinement. The first results on Lambda baryon production in medium-size systems, such as Ar+Sc, are presented with a focus on the methodology employed in the analysis. They are compared with available world data from proton-proton and nucleus-nucleus collisions, and selected theoretical models.

*42nd International Conference on High Energy Physics (ICHEP2024)*

*18-24 July 2024*

*Prague, Czech Republic*

---

\*Speaker

## 1. Introduction

The study of quark-gluon plasma (QGP) properties remains a major focus in high-energy heavy-ion physics, driven by the assumption that this state of matter existed in the early Universe. Additionally, the study of QGP has implications for astrophysical research related to neutron stars, as extreme densities could potentially result in the QGP formation inside their cores. As a result, numerous theoretical and experimental efforts are made in order to understand the conditions under which QGP is created and map the phase diagram of strongly interacting matter.

One of the earliest proposed signatures of QGP formation is strangeness enhancement [1]. It was confirmed by a plethora of heavy-ion experiments at CERN Super Proton Synchrotron (SPS). For instance, the results from lead-lead collisions by NA49 experiment [2] are illustrated in Fig. 1. It shows the energy dependencies of the ratio of the mean multiplicities of kaons and pions and the strangeness enhancement factor  $E_S$ . The latter is defined as  $E_S = \frac{\langle \Lambda \rangle + \langle K + \bar{K} \rangle}{\langle \pi \rangle}$ , where  $\langle \pi \rangle$  is equal to  $1.5 \cdot (\langle \pi^+ \rangle + \langle \pi^- \rangle)$ , and  $\langle \pi^+ \rangle$  and  $\langle \pi^- \rangle$  are multiplicities of positively and negatively charged pions, respectively. A steep rise in both quantities at AGS energies is observed, followed by a peak and subsequent plateau for RHIC energies, contrary to the results from p+p collisions, where no peak is found.

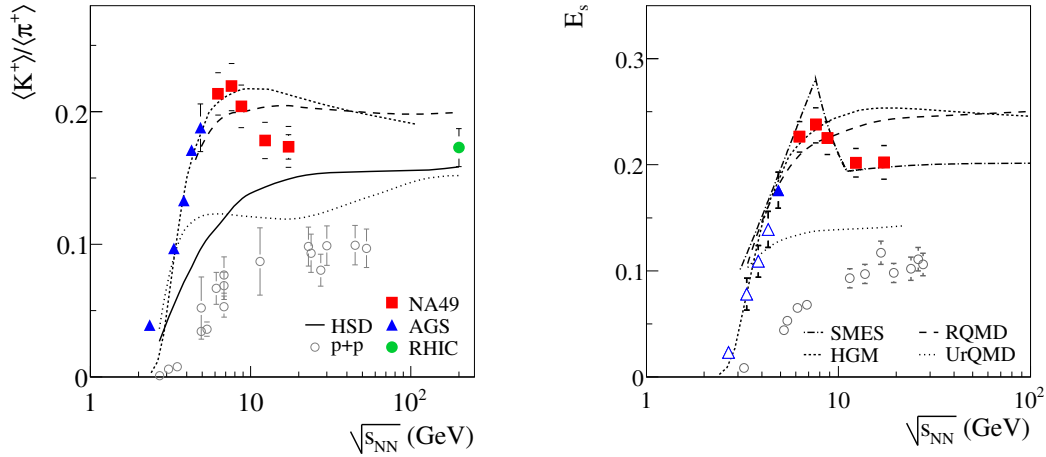


**Figure 1:** Energy dependence of  $\langle K^+ \rangle / \langle \pi^+ \rangle$  ratio (left) and strangeness enhancement  $E_S$  (right, see text for further details) measured by the NA49 experiment [2].

Current efforts focus on exploring energy and system-size dependencies of the strangeness enhancement. Particularly, results from medium-size collision systems are important, since they bridge the gap between small (p+p) and large (Au+Au and Pb+Pb) systems, and yet, the present data is rather scarce and limited to multiplicities at mid-rapidity. Such studies are critical for refining theoretical models of particle production.

## 2. NA61/SHINE detector

NA61/SHINE is a fixed-target experiment located at the H2 beamline in CERN's North Area [4], which uses the beams from the SPS. The experiment focuses on studying the QCD phase diagram

by measuring charged and neutral hadron production across a broad range of collision energies and system sizes. A schematic diagram of the NA61/SHINE detector is illustrated in Fig. 2.

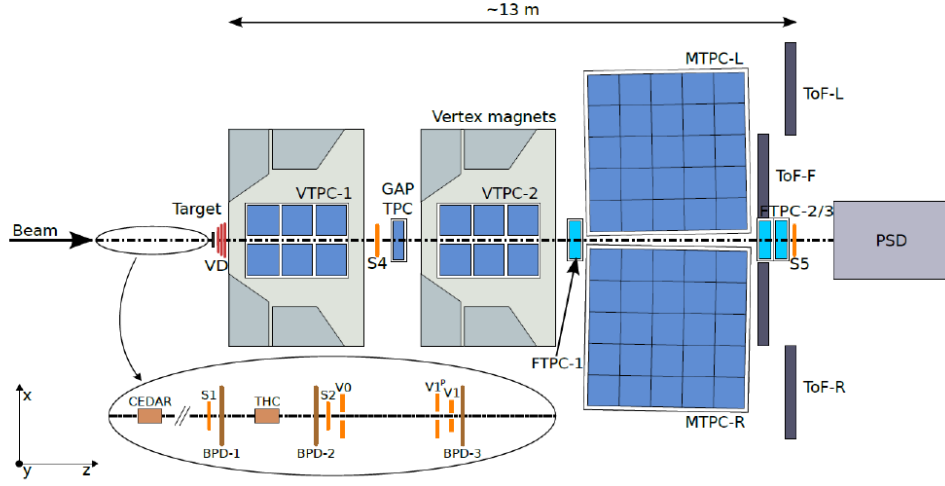


**Figure 2:** Schematic view of the NA61/SHINE detector.

Upstream from the target, the beam position detectors are utilized to monitor the composition and trajectory of the incoming beam. Particle identification and momentum measurement are done using data from a set of Time Projection Chambers, two of which are placed within the magnetic field of superconducting dipole magnets, as well as Time-of-Flight detectors. The Projectile Spectator Detector (PSD) is a forward calorimeter that measures energy along the beam direction. In nucleus-nucleus collisions, this measurement primarily reflects the number of beam projectile spectators (non-interacting nucleons), allowing the determination of the collision centrality.

### 3. Results

New preliminary results on  $\Lambda$  baryon production in 0–10% central Ar+Sc collisions at 40A and 150A GeV/c ( $\sqrt{s_{NN}} = 8.77$  and 17.3 GeV, respectively), which include rapidity spectra (in the center-of-mass frame) and the mean multiplicities, are shown along with earlier released data for 75A GeV/c ( $\sqrt{s_{NN}} = 11.9$  GeV) [5]. In this analysis,  $\Lambda$  baryons are identified through their weak decay channel,  $\Lambda \rightarrow p\pi^-$  (branching ratio of 63.9%). Their yield is estimated by fitting to the invariant mass of track pairs. The results are corrected for losses due to the detector's geometrical acceptance, reconstruction inefficiencies, selection criteria applied during the analysis, branching ratio, and feed-down from the decays of heavier hyperons. A more detailed description of the analysis methodology is available in Ref. [6].

The one-dimensional transverse momentum spectra are fitted using an exponential function  $f(p_T) = A \cdot p_T \cdot \exp\left(\frac{\sqrt{p_T^2 + m_\Lambda^2}}{T}\right)$ , where  $A$  is a normalization factor,  $p_T$  is a transverse momentum,  $m_\Lambda$  is the  $\Lambda$  baryon rest mass, and  $T$  is an inverse slope parameter, with  $T$  and  $A$  being the fit parameters. Fitting is used to extrapolate the spectra to the unmeasured  $p_T$  region. The resulting one-dimensional rapidity spectra are shown in Fig. 3, alongside the predictions of the EPOS

1.99 [7] and the SMASH [8] models, both of which underestimate the  $\Lambda$  production at analyzed beam momenta.

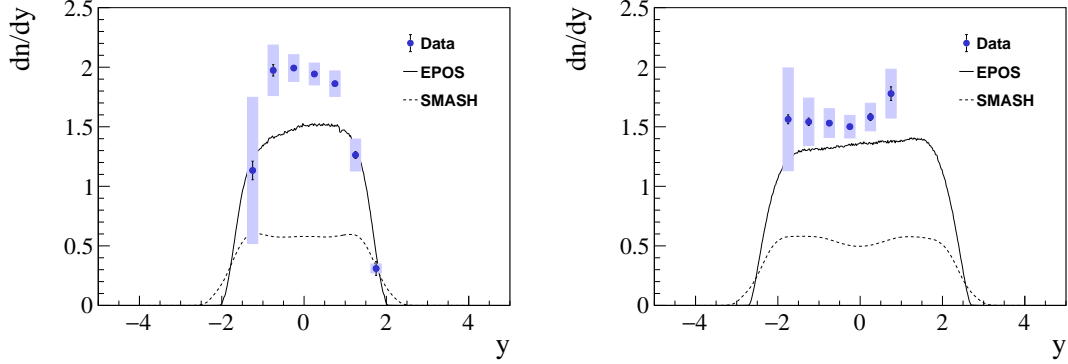


**Figure 3:** Comparison of rapidity spectra of  $\Lambda$  baryons produced in central Ar+Sc collisions at 40A (*left*) and 150A GeV/c (*right*) with predictions of EPOS 1.99 [7] and SMASH [8] models. The statistical uncertainties are depicted as vertical bars, while the systematic uncertainties are presented as shaded boxes.

The mean multiplicities  $\langle\Lambda\rangle$  are determined by summing the measured values scaled under the assumption that the yield ratio between measured and unmeasured regions is consistent between the experimental data and the EPOS model. The mean multiplicities of  $\Lambda$  baryons obtained are  $5.49 \pm 0.12$  (stat.)  $\pm 0.24$  (sys.) for Ar+Sc at 40A GeV/c and  $6.43 \pm 0.13$  (stat.)  $\pm 0.88$  (sys.) for Ar+Sc at 150A GeV/c. The resulting values are compared with model predictions in Fig. 4. The EPOS 1.99 model [7] tends to underestimate both mid-rapidity yield ( $|y| < 0.5$ ) and mean multiplicity, although its predictions come closer to the experimental results at the highest energy. In contrast, the SMASH model [8] consistently predicts significantly lower values for both quantities across the entire energy range.

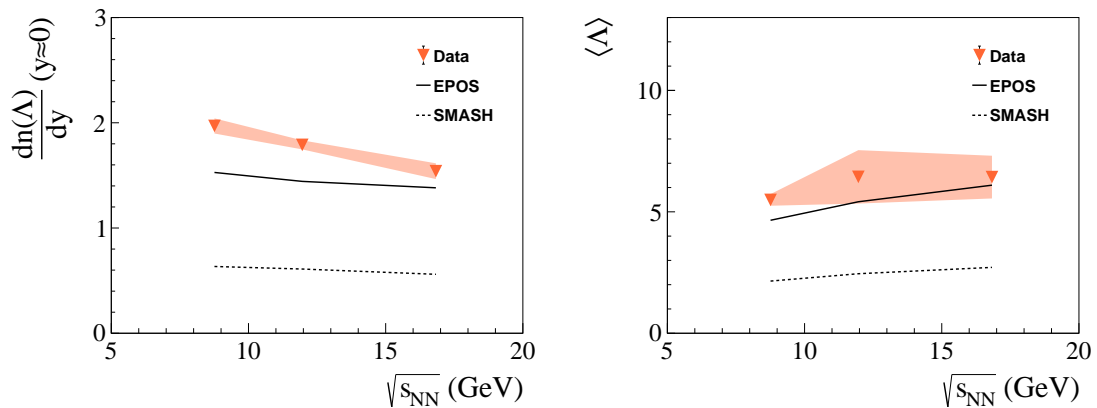


**Figure 4:** Comparison of the energy dependence of mid-rapidity multiplicities (*left*), and mean multiplicities (*right*) of  $\Lambda$  baryons produced in central Ar+Sc collisions at 40A, 75A, and 150A GeV/c with predictions of EPOS 1.99 [7] and SMASH [8] models. The systematic uncertainties are presented as a shaded band.

Figure 5 shows the energy dependencies of the mid-rapidity yield and the mean multiplicity of  $\Lambda$  baryons, alongside existing world data. Across the SPS energy range, both quantities appear to reach a plateau, regardless of the system size. The values for Ar+Sc and Si+Si collisions are notably closer to those observed in Au+Au and Pb+Pb collisions than to those in p+p interactions.

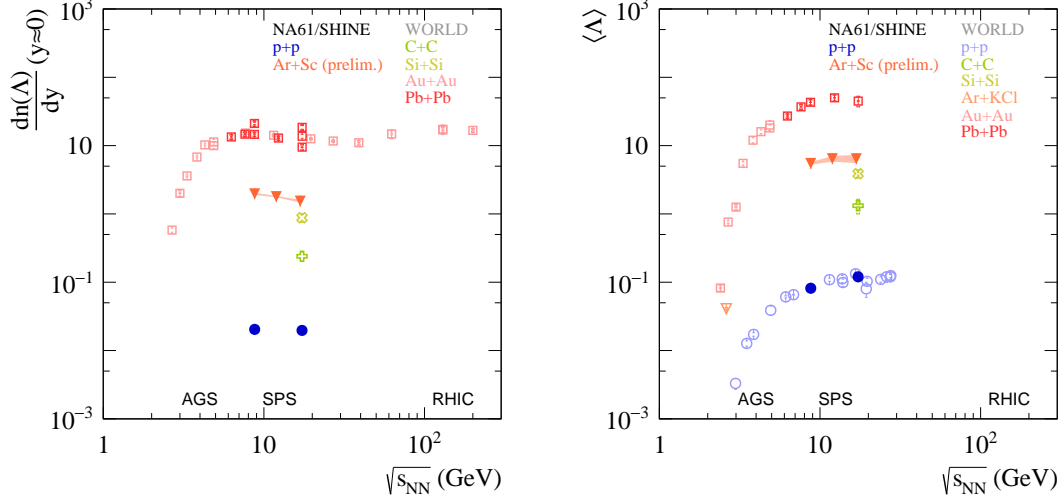


**Figure 5:** The energy dependence of mid-rapidity yield (*left*) and the mean multiplicity (*right*) of  $\Lambda$  baryons. The systematic uncertainties of the Ar+Sc results are presented as a shaded band. Results for p+p, Ar+Sc, Ar+KCl, C+C, Si+Si, Au+Au, and Pb+Pb are shown. See the supplementary material for the references to the world data.

Figure 6 presents the energy dependence of the  $\langle\Lambda\rangle/\langle\pi\rangle$  ratio and the strangeness enhancement,  $E_S$ , following the description given earlier in the text. At SPS energies, the  $\bar{\Lambda}/\Lambda$  ratio is typically below 0.15 [2], so the  $\bar{\Lambda}$  contribution to  $E_S$  is considered negligible. For p+p data,  $\langle K + \bar{K} \rangle$  is taken as  $4 \cdot \langle K_S^0 \rangle$ , while for A+A data, it is expressed as  $2 \cdot (\langle K^+ \rangle + \langle K^- \rangle)$ . In case of Au+Au and Pb+Pb collisions, both the  $\langle\Lambda\rangle/\langle\pi\rangle$  ratio and  $E_S$  exhibit a clear maximum at intermediate SPS energies, while no maximum is observed in the results for lighter systems, including Ar+Sc. At the same time, the  $\langle\Lambda\rangle/\langle\pi\rangle$  ratio for Ar+Sc collisions across the three studied energies shows a trend similar to that in the heavier Pb+Pb system.

#### 4. Acknowledgements

This work was supported by the funds granted under the Research Excellence Initiative of the University of Silesia in Katowice and by the Polish Minister of Education and Science (contract No. 2021/WK/10).

#### References

- [1] J. Rafelski and B. Muller, *Strangeness Production in the Quark - Gluon Plasma*, *Phys. Rev. Lett.* **48** (1982), 1066, [erratum: *Phys. Rev. Lett.* **56** (1986), 2334]

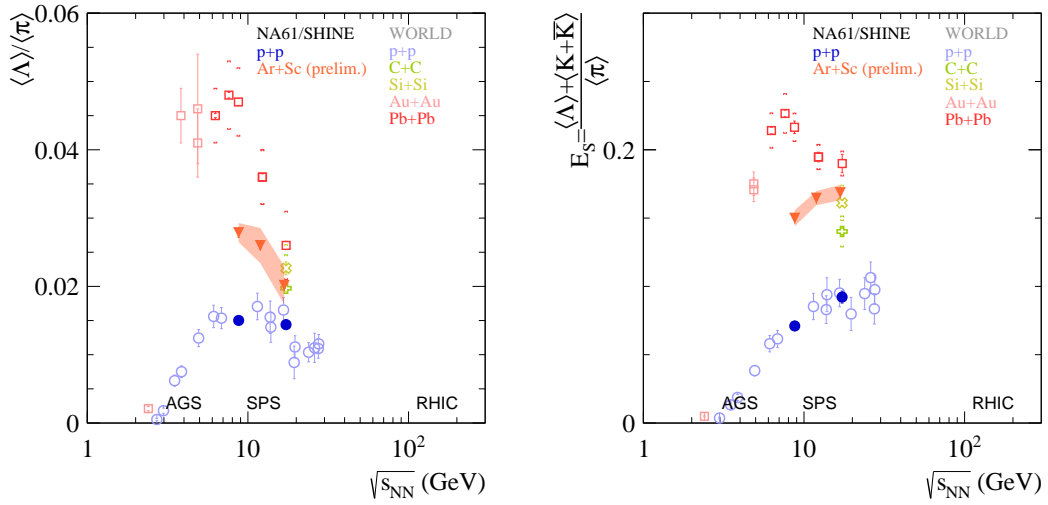


**Figure 6:** The energy dependence of  $\langle \Lambda \rangle / \langle \pi \rangle$  ratio (left) and strangeness enhancement  $E_S$  (right). The systematic uncertainties of the Ar+Sc results are presented as a shaded band. Results for p+p, Ar+Sc, C+C, Si+Si, Au+Au, and Pb+Pb are shown. See the supplementary material for the references to the world data.

- [2] C. Alt *et al.* [NA49 Coll.], *Pion and kaon production in central Pb + Pb collisions at 20 A and 30 A GeV: Evidence for the onset of deconfinement*, *Phys. Rev. C* **77** (2008), 024903, [arXiv:0710.0118 [nucl-ex]].
- [3] M. Gazdzicki and M. I. Gorenstein, *On the early stage of nucleus-nucleus collisions*, *Acta Phys. Polon. B* **30** (1999), 2705, [arXiv:hep-ph/9803462 [hep-ph]].
- [4] N. Abgrall *et al.* [NA61 coll.], *NA61/SHINE facility at the CERN SPS: beams and detector system*, *JINST* **9** (2014), P06005 [arXiv:1401.4699 [physics.ins-det]].
- [5] Y. Balkova [NA61 Coll.], *Strangeness Production in Heavy-ion Collisions at the NA61/SHINE Experiment*, *Acta Phys. Polon. Supp.* **17** (2024) no.3, 3-A20
- [6] Y. Balkova [NA61 coll.], *Strangeness production in the NA61/SHINE experiment at the CERN SPS energy range*, *Frascati Phys. Ser.* **72** (2022), 60-65.
- [7] T. Pierog and K. Werner, *EPOS Model and Ultra High Energy Cosmic Rays*, *Nucl. Phys. B Proc. Suppl.* **196** (2009), 102-105, [arXiv:0905.1198 [hep-ph]].
- [8] J. Mohs *et al.* [SMASH Coll.], *Particle Production via Strings and Baryon Stopping within a Hadronic Transport Approach*, *J. Phys. G* **47** (2020) no.6, 065101, [arXiv:1909.05586 [nucl-th]].